Intrinsic Deformation Behavior of Semicrystalline Polymers

Bernard A. G. Schrauwen, Roel P. M. Janssen, Leon E. Govaert,* and Han E. H. Meijer

Dutch Polymer Institute (DPI), Section Materials Technology (MaTe), Eindhoven University of Technology, P.O. Box 513, NL-5600MB, Eindhoven, The Netherlands

Received August 28, 2003; Revised Manuscript Received May 28, 2004

ABSTRACT: The influence of crystallinity and lamellar thickness on the intrinsic deformation behavior of a number of semicrystalline polymers is studied: a poly(ethylene terephthalate) and two different molecular weight grades of polyethylene and polypropylene. The crystallinity and lamellar thickness are altered by varying the rate of crystallization from the melt and by cold crystallization (annealing) at elevated temperatures above T_g but below the melting point. Crystallinity and lamellar thickness are determined by wide-angle X-ray diffraction and small-angle X-ray scattering measurements. Uniaxial compression tests are performed to obtain the large strain intrinsic deformation behavior, e.g., yield stress, strain softening, and strain hardening modulus. The yield stress is found to be proportional to lamellar thickness, whereas the strain hardening modulus is shown not to depend on crystallinity or lamellar thickness. Over the strain range experimentally covered, the strain hardening modulus appears to be well described by a simple neo-Hookean relation and appears to be related to the chain entanglement density. An affirmation for this relation arises from the observation that slowly melt crystallized samples exhibit a lower strain hardening, resulting from a lower chain entanglement density, which is expected to be caused by reeling in of the molecular chains in such a slow crystallization process. The similarity in the results observed on all polymers tested supports the conclusion that the crystalline phase does not contribute to strain hardening, which is primary controlled by the chain entanglement density.

1. Introduction

The search for a relationship between molecular structure and mechanical properties of semicrystalline polymers has been a motive for extensive studies in the past. The problems in understanding the deformation of semicrystalline polymers arises from the presence of a two-phased structure, and a tendency exists in concentrating primarily on the behavior of the crystalline regions. Elasticity (Young's modulus) appears to be understood, in a qualitative sense, in terms of a relation between volume fraction of crystalline and amorphous domains,[1,2] but extensive discussion proceeds in finding an explanation of the effect of crystallinity on yield stress and strain hardening. Both properties have been studied on a wide range of semicrystalline polymers but are concentrated mainly on polyethylene- and ethylene-based copolymers. In achieving an as large as possible variation in crystallinity and lamellar thickness, characteristics like number of branches, molecular weight, and type of comonomer were varied. The type of crystallization procedures were changed, ranging from solution to melt crystallization and annealing processes at different concentrations, cooling rates, and temperatures. Generally all these parameters were changed to find an explanation for the influence of one parameter only: the crystalline structure. Maybe this caused the various hypotheses that were presented to explain the behavior observed.

Strain hardening of a number of thermoplastic polymers was studied by G'Sell et al.,[3,4] who constructed true stress−strain curves from tensile experiments performed at a local constant strain rate, controlled by in-situ measurement of the diameter in the neck. Strain hardening was proposed to originate from the molecular entanglement network by Haward and Thackray,[5] who used a constitutive model in which a rubber-elastic response was incorporated. The Gaussian description of the strain hardening modulus proved to be valid for all thermoplastic polymers studied in a review by Haward[6] and was also successfully used to describe the strain hardening up to high draw ratios ($\lambda = 3$) in amorphous PC[7] and in cross-linked PS and blends of PS and PPO.[8] In the Gaussian theory, the strain hardening is proportional to the network density and absolute temperature. The proportional relation between the strain hardening modulus, measured in compression, and the entanglement (network) density observed by Van Melick et al.[8] for PS/PPO blends is in agreement with these earlier findings. A physical support for the rubber-elastic approach is the reversibility of plastic deformation when deformed amorphous polymers are brought above their glass transition temperature.[9] On the other hand, a disagreement with the Gaussian behavior of rubber-elasticity is the observed negative temperature dependence,[8,10] since the modulus of a true entropic spring would increase with temperature. The negative temperature dependence was suggested to be, at least partly, related to the stress-induced segmental mobility of chains.[8] For this reason, neo-Hookean behavior is preferred over Gaussian behavior.

Large strain deformation of semicrystalline polymers is usually discussed in terms of the molecular network, represented by trapped chain entanglements in the amorphous phase and crystallites acting as physical cross-links.[12−14] The influence of the number of trapped entanglements on ultradrawability of high molecular weight polyethylene was considered in studies by Smith and Lemstra.[15−17] The maximum attainable draw ratio was found to increase with decreasing initial polymer concentration in solution-crystallized films and was discussed in terms of a reduced entanglement density in the solid state.[15,16] Furthermore, a pronounced concomitant decrease in strain hardening was observed in

* Corresponding author. E-mail L.E.Govaert@tue.nl.

10.1021/ma035279t CCC: $27.50
Published on Web 07/07/2004

the nominal stress−strain curves of the solution-crystallized films.[16] True stress−strain curves showed that the strain hardening modulus of melt-crystallized films was significantly larger than observed for solution-cast films, and partial remelting of the solution-cast film resulted in an intermediate level of strain hardening.[17] Also, a decrease in strain hardening was found for increasing testing temperatures.

All tensile tests on these high molecular weight polyethylene samples were performed in a temperature range above the α-relaxation temperature, where crystals are known to yield readily, and an influence of crystallites acting as physical cross-links (i.e., the contribution of tie molecules on the network) was considered to be absent.[16] Hiss et al.[13] studied the true stress−strain behavior at room temperature, obtained by video-controlled tensile tests, up to large strains of various polyethylenes and related copolymers. They also used the neo-Hookean model to determine the strain hardening modulus. An increase in strain hardening was observed with increasing crystallinity, which was rationalized by an effective contribution, to the network density, of chains anchored in adjacent crystallites. However, the degree of crystallinity was not the only parameter that was varied in the study concerned, as also molecular weight and branching were varied in order to obtain the differences in crystallinity. It can be expected that these differences in molecular structure also influence the strain hardening. For example, the number of entanglements per molecule increases with molecular weight and should therefore also be considered to effect the strain hardening. Studies by Kennedy et al.[18,19] on linear polyethylene and random copolymers of ethylene with narrow molecular weight distributions indeed indicate a relation between entanglement density and strain hardening modulus. The influence of molecular weight, branch content, and branch type was investigated, but a less strenuous mechanism, being strain-induced crystallization, was presented in explaining strain hardening. From all reviewed results, the exploitation of the concept of the rubber-elasticity theory, i.e., strain hardening being proportional to entanglement density, seems to be most plausible for semicrystalline polymers.

Concerning the yield stress in semicrystalline polymers, there still does not seem to be a perfectly understood qualitative explanation in terms of morphological characteristics. In the early days, a dependency of yield stress on the degree of crystallinity was recognized. Since a glassy amorphous phase also exhibits yielding, most of the studies focus on polyethylene tested above the glass transition temperature, with the amorphous part exhibiting rubberlike behavior, hence displaying no yield. Popli and Mandelkern[20] reported a linear relation between lamellar thickness and yield stress. In their study, molecular weight and spherulitic superstructure were found not to have any influence on the yield stress. The proportional relation between lamellar thickness and yield was assigned to the process of partial melting and recrystallization.[21] Another, more accepted, approach in explaining the yield stress in semicrystalline polymers follows from the classical ideas of crystal plasticity, considering that nucleation and propagation of dislocations control yielding. Young[22,23] developed a model in which the yield stress is determined from the energy to nucleate a screw dislocation within the crystalline lamellae, resulting in a direct model relation between lamellar thickness and yield stress. A number of authors[24−29] validated this model by experimental testing, using experimental and theoretical obtained values for the unknown parameters from literature. While some authors only found the theory to predict a correct order of magnitude of the experimentally obtained yield stress,[24] others showed a good agreement between theory and experiments.[25−27] It is probably the inconsistency in the use of several of the parameters of the model which caused these differences. But the above approaches in understanding the yield mechanism are not based on kinetic aspects, and some discussion in the use of several "unknown" parameters and the explanation of observed results is present. A new approach to the model of nucleation of screw dislocations was brought up by Séguéla,[30] who proposed that the driving force for nucleation and propagation of dislocations relies on the thermally activated conformational (chain twist) defects.

Table 1. Characteristics of Polymer Grades Used in This Study

material	trade name	M_w [g mol^{-1}]	M_n [g mol^{-1}]
PE-1	Stamylan HD 9089S	70 000	11 000
PE-2	Stamylan HD 8621	210 000	7 000
PP-1	Stamylan P 17M10	260 000	57 000
PP-2	Stamylan P 13E10	500 000	84 000
PET	Arnite-D	76 000	36 200

The use of uniaxial compression tests, performed at constant logarithmic strain rate, looks a promising route[8] to measure the large strain behavior of polymers. The motivation of this study is finding a relationship between the crystalline structure and the intrinsic mechanical deformation of semicrystalline polymers, measured in compression. A set of three different polymers is chosen to be investigated: high-density polyethylene, polypropylene, and poly(ethylene terephthalate). Crystalline structures are mainly changed by annealing processes of quenched samples, also called cold crystallization for poly(ethylene terephthalate). A highlight of this study is the strain hardening behavior of the polymers under investigation, whereas yielding will only be investigated for the most commonly studied polymer: polyethylene. The results should mainly supply a basis for a proper understanding of the strain hardening behavior.

2. Experimental Section

2.1. Materials. The semicrystalline polymers used in this study can be distinguished in three types regarding their glass transition temperature (T_g): high-density polyethylene (HDPE), with $T_g < T_{room}$, polypropylene (PP), with $T_g \approx T_{room}$, and poly(ethylene terephthalate) (PET), with $T_g > T_{room}$. For PE and PP two grades were selected differing in molecular weight, as given in Table 1. All polymers were supplied by DSM, The Netherlands. The Arnite-D PET grade is a postcondensated product of the commercial grade D00-300 and contains 2 mol % isophetalic acid, resulting in a decrease of crystallization rate facilitating the control in degree of crystallinity.

2.2. Sample Preparation. The materials were compression-molded between brass plates and aluminum foil into a mold of 150 × 75 × 5 mm^3 at suitable temperatures (200, 220, and 280 °C for respectively HDPE, PP, and PET), imposed by the two heating plates of the press. The polymer pellets were first completely melted under atmospheric pressure, and subsequently the pressure was increased stepwise to a maximum pressure of approximately 500 kPa. Degassing, by means of releasing the pressure, was not applied to prevent contact of the surrounding air to the polymer melt, which increases the chance of polymer degradation, especially in the case of

Table 2. Characteristics of Crystallization Procedures

material	code	cooling melt	isothermally	X [%]	X_{vol} [%]	D [nm]	L_c [nm]
PET	Q15	15 °C		0	0		
	IC100h4	15 °C	4 h @ 100 °C	0	0		
	IC100h24	15 °C	24 h @ 100 °C	11.6	10.4		
	IC100h72	15 °C	72 h @ 100 °C	27.1	24.8	10.5	2.6
	IC110m15	15 °C	15 min @ 110 °C	21.7	19.7		
	IC110h4	15 °C	4 h @ 110 °C	26.4	24.1	11.9	2.9
	IC110h54	15 °C	54 h @ 110 °C	29.1	26.7	10.2	2.7
	C135	135 °C		31.4	28.9	13.4	3.9
	C150	150 °C		32.2	29.6	13.5	4.0
	C200	200 °C		34.7	32.0	16.8	5.4
	SC	in press		42.6	39.6	16.1	6.4
PE-1	Q15	15 °C		68.4	64.8	26.7	17.8
	IC100h8	15 °C	8 h @ 100 °C	69.9	66.4	27.4	18.2
	IC100h24	15 °C	24 h @ 100 °C	71.0	67.5	27.3	18.4
	IC100h48	15 °C	48 h @ 100 °C	73.3	70.0	29.4	20.6
	IC100h72	15 °C	72 h @ 100 °C	73.8	70.5	29.6	20.9
	IC110h8	15 °C	8 h @ 110 °C	72.3	68.9	29.0	20.0
	IC110h48	15 °C	48 h @ 110 °C	73.5	70.2	29.5	20.7
	IC120h8	15 °C	8 h @ 120 °C	74.1	70.9	31.4	22.3
	IC120h24	15 °C	24 h @ 120 °C	75.6	72.5	32.4	23.5
	IC120h48	15 °C	48 h @ 120 °C	76.5	73.5	32.7	24.0
	IC125h8	15 °C	8 h @ 125 °C	75.6	72.5	34.7	25.2
	IC125h48	15 °C	48 h @ 125 °C	76.6	73.6	35.9	26.4
	SC	in press		76.7	73.7	36.7	27.0
PE-2	Q15	15 °C		68.4	64.8	29.9	19.4
	IC125h48	15 °C	48 h @ 125 °C	72.9	69.6	40.2	28.0
	SC	in press		73.8	70.5	40.5	28.6
PP-1	Q15	15 °C		69.3	66.9	19.2	12.8
	IC140	15 °C	4 h @ 140 °C	72.8	70.5	22.6	15.9
	SC	5 h @ 140 °C		73.5	71.3	23.8	17.0
PP-2	Q15	15 °C		68.2	65.7	19.3	12.7
	IC140	15 °C	4 h @ 140 °C	69.9	67.5	23.4	15.8
	SC	5 h @ 140 °C		73.4	71.2	25.2	17.9

PET. To avoid hydrolysis, PET was dried in a vacuum oven for at least 10 h at 110 °C before molding. The polymers were kept at the applied pressure and temperature for at least 15 min in order to create homogeneous samples, minimizing the effect of thermal history. The samples were subsequently subjected to different crystallization procedures in order to obtain different levels of crystallinity and lamellar thickness. Within these procedures two types can be distinguished: crystallization coming from above and coming from below the melting temperature.

The procedures applied from above the melting temperature for PE and PET consisted of either placing the molten samples in a cold press of 15 °C (quenching, Q15) after removing the brass plates in order to achieve the highest possible cooling rate of about 12−22 °C/s or leaving the molten samples in the press turning off the heat source (slow cooling, SC), allowing to cool to room temperature at a rate of about 0.01 °C/s. For the PET samples intermediate cooling rates were also applied, placing the samples in a hot press at 200 °C (C200), 150 °C (C150), and 135 °C (C135). Cooling rates for these temperatures were not measured and assumed to decrease for increasing temperature of the hot "cooling" press. With respect to the crystallization temperature these types of "fast" and "slow" cooling of PE and PET can be considered as nonisothermal. The "fast" cooling technique (Q15) was also applied to PP, but for "slow" crystallization the samples were isothermally crystallized by placing the hot melt in a hot press at 140 °C for at least 5 h. Although, these samples are coded as "slow cooling" (SC), it should be considered that this is an isothermal crystallization procedure, since the crystallization of PP now fully takes place at the temperature of 140 °C.

The second type of crystallization procedures were all isothermal (isothermal crystallization, IC) and were only applied to the "quenched" samples (cooled at 15 °C). For PET this isothermal crystallization procedure is known as "cold" crystallization, and for PE and PP it is known as an annealing process. The samples were wrapped in aluminum foil, sealed with adhesive Teflon tape, and placed in a temperature-controlled silicon oil bath at given annealing temperatures for different times. This annealing of the quenched samples resulted in an increase of the crystalline long period, given by[31]

$$D(t) = D_0 + B(T)\ln\left[\frac{t}{t_0}\right] \qquad t_0 > 0 \tag{1}$$

where D is the long period at time t, D_0 is the initial long period of the unannealed sample at a corresponding positive but very small time t_0, and $B(T)$ is a constant which is a function of temperature T. From this equation it follows that, upon annealing, the crystalline long period depends on the time and temperature of annealing. Times and temperatures of all isothermal crystallization procedures applied are given in Table 2. For the uniaxial compression tests, cylindrical samples (4 mm × 4 mm) were machined from the plates.

2.3. Crystallinity and Lamellar Thickness. The degree of crystallinity and the lamellar thickness were measured by wide- and small-angle X-ray scattering experiments, respectively. Samples with a thickness of about 2 mm, cut from the plates, were used to measure simultaneously 2D SAXS and a 1D WAXS patterns at the Dutch-Belgium beamline (DUBBLE, CRG BM26) at the European Synchrotron Radiation Facility (ESRF) in Grenoble, France. The size of the beam was 1 × 0.3 mm^2, X-ray wavelength was 1.24 Å, and sample-to-detector distance for SAXS measurements was 4 m. The 1D WAXS detector was calibrated using the known peak positions of HDPE for the given wavelength using Bragg's law:

$$n\lambda = 2d\sin\theta \tag{2}$$

Figure 1a shows an example of a WAXS profile of an amorphous and semicrystalline PET sample. Both profiles are scaled to the same intensity at a 2θ angle of 15.5°, and background scattering is subtracted in order to determine the weight fraction of crystals of the semicrystalline sample using

$$\chi = \frac{C - A}{C} \tag{3}$$

where C is the area of the crystalline profile and A is the area

of the amorphous profile. In the case of the PET samples the amorphous halo is assumed to be measured for the fast cooled samples, since no peaks are observed on the broad halo of these profiles (see Figure 1a). The amorphous WAXS halo of polypropylene was obtained from ref 32. For polyethylene the amorphous scattering is almost impossible to measure due to a fast crystallization rate. Therefore, an amorphous halo was only estimated, giving an approximation of the degree of crystallinity.[33]

The crystalline long period, D, which is related to the distance between lamellae, was determined from the SAXS measurements. The 2D SAXS data were divided by the detector response obtained from uniform illumination of a Cu source, and background scattering was subtracted. Subsequently, the patterns were circumferentially integrated in radial direction, resulting in 1D SAXS profiles (see for example Figure 1b). The applied integration inherently gives a q^2 multiplication to the intensity, which takes care of the Lorentz correction and allows the SAXS profiles to be used for determination of the lamellar spacing. Since sample thickness varied and beam intensity fluctuated during the experiments, a scaled intensity is plotted against the scattering vector q, which is defined as

$$q = \frac{2\pi}{D} = \frac{4\pi}{\lambda}\sin\theta \tag{4}$$

where D is the lamellar long spacing, λ the X-ray wavelength, and θ the scattering angle. The scattering angle can be calculated from the position of the scattered intensity on the detector and the sample-to-detector distance, which was calibrated accurately using the scattering pattern of a dry rat tail collagen. The peak position of the SAXS profiles are taken to calculate the average lamellar thickness from

$$L_c = \chi_{vol} D \tag{5a}$$

where χ_{vol} is the volumetric percentage of crystallinity calculated from the crystal weight percentage χ:

$$\chi_{vol} = \frac{\frac{\chi}{\rho_C}}{\frac{\chi}{\rho_C} + \frac{100-\chi}{\rho_A}} \times 100\% \tag{5b}$$

where χ was obtained from the WAXS profiles, ρ_C is the crystal density, and ρ_A is the amorphous density. The values for the amorphous and crystalline densities where adopted from Van Krevelen[34] (PE: $\rho_C = 1.0$ g/cm^3, $\rho_A = 0.85$ g/cm^3; PP: $\rho_C = 0.95$ g/cm^3, $\rho_A = 0.85$ g/cm^3; PET: $\rho_C = 1.5$ g/cm^3, $\rho_A = 1.33$ g/cm^3).

2.4. Mechanical Testing. Compression tests were performed on a servo-hydraulic MTS Elastomer Testing System 810 at room temperature. Cylindrical specimens (4 mm × 4 mm) were compressed at a constant logarithmic strain rate of 3×10^{-3} s^{-1} between two parallel, flat steel plates. The friction between the sample and steel plates was reduced by an empirically optimized method: onto the sample a thin film of PTFE tape (3M 5480, PTFE skived film tape) was applied, and the surface between steel and tape was lubricated by a soap−water mixture. During compression tests no bulging or buckling of the samples was observed, indicating that the friction was sufficiently reduced. To achieve a true logarithmic strain rate, the displacement of the steel plates was controlled by an extensometer. True stress−strain curves could be constructed from the measured force and displacement, by assuming that the deformation applied was volume invariant.

3. Results and Discussion

3.1. Crystallinity and Lamellar Thickness. The crystallinity χ, long spacing D, and lamellar thickness L_c for each sample are shown in Table 2. As expected, the degree of crystallinity was found to be lowest for the quenched (Q15) samples and highest for the slowly cooled samples (SC) for all polymers used. The isothermal crystallization procedures were applied to successfully obtain intermediate levels of crystallinity and lamellar thickness for the PET and PE-1 samples. For the longest annealing times, the maximum lamellar thickness depends on the annealing temperature, which was also anticipated from the term $B(T)$ of eq 1. Although the annealing temperature applied to the PET samples was not sufficient to get a lamellar thickness equal to the slowly cooled melt-crystallized sample (PET SC), for the low molecular weight HDPE, a complete range in crystallinity and lamellar thickness was reached. Here isothermal crystallization at 125 °C for 48 h resulted in almost similar values as the slowly cooled samples. But it should be considered that the isothermal crystallization temperature of 125 °C is very close to the melting temperature of HDPE, and therefore it could well be possible that these samples were partially remelted and crystallized at this elevated temperature close to the melt. An indication for this can also be found in Figure 1b, where the SAXS profiles are plotted for several PE-1 samples. Here it can be seen that not only the average long spacing but also the deviation in long spacing for these two crystallization procedures is fairly similar. Comparison of the intensity levels of the different SAXS profiles for proper interpretation is dangerous since the sample thickness was not constant and influences the intensity due to absorption.

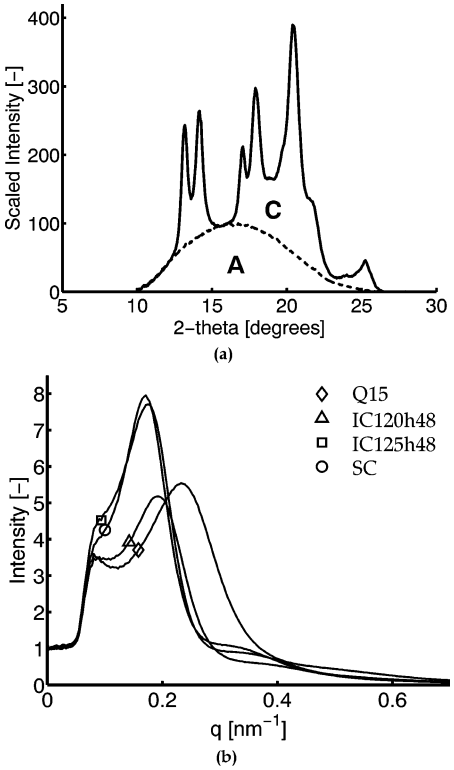

Figure 1. WAXS profiles of amorphous (A: Q15) and crystalline (C: SC) PET (a) and SAXS profiles of several PE-1 samples (b).

A relation seems to be present between the degree of crystallinity and lamellar thickness for each polymer. For the low crystalline PET samples the lamellar thickness could not be obtained from the SAXS patterns. The highest isothermal crystallization temperature of 110 °C applied to the PET samples was not sufficient to reach a maximum level of crystallinity, as obtained

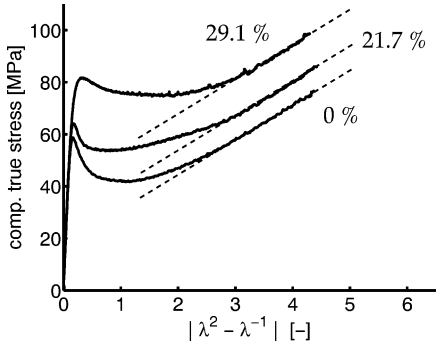

Figure 2. Compressive behavior of isothermally crystallized PET samples, having different degree of crystallinity (χ).

for the melt crystallized samples. So, unfortunately, the isothermally crystallized samples do not cover the complete possible range of crystalline characteristics. Nevertheless, PET is an attractive polymer to investigate since the variation of the crystallinity obtained is relatively large, ranging from completely amorphous to 42.6% crystalline. Therefore, the intrinsic behavior of PET will be briefly discussed first in the following section since the differences between semicrystalline and amorphous behavior of PET can be easily observed.

3.2. Intrinsic Behavior. The intrinsic compressive behavior of three different PET samples, with different degree of crystallinity obtained via isothermal crystallization procedures, is given in Figure 2. For the amorphous PET sample ($\chi = 0\%$) a behavior typical for glassy polymers is observed: an initial elastic region followed by a yield stress after which intrinsic strain softening ("yield drop") and strain hardening occurs. Increasing the crystallinity results in an increase in yield stress and a decrease in yield drop. Apparently, the crystalline domains contribute more to the yield stress than the amorphous part, resulting in a larger total yield stress of the material. Moreover, if the amount of amorphous polymer decreases, the yield drop, which is an amorphous property,[35] is observed to decrease.

3.3. Strain Hardening. *PET.* From the true stress−true strain compression curves the strain hardening modulus can be determined at large strains, and following a neo-Hookean description, which was found to be valid for most polymers,[6,11] at large strains the stress should be proportional to $\lambda^2 - \lambda^{-1}$. In Figure 2 the true stress is plotted vs this strain measure, and the strain hardening modulus is defined as the slope at large strains ($\lambda \sim 2$), drawn as the dashed lines. Considering the Gaussian background of the neo-Hookean behavior, the strain hardening modulus is related to the entanglement (network) density, which was experimentally proven to be valid for amorphous polymers,[7,8] including PET (see Figure 2). Crystallizing the amorphous PET, by isothermal ("cold") crystallization, increases the connectivity in the polymer, resulting in an increase of the yield stress. However, the strain hardening modulus of the crystallized samples is found to be equal to that of the amorphous sample and is clearly not related to the degree of crystallinity. Apparently, after yield the crystallites no longer form physical junction points, and essential chain transport through the crystal is possible. As a result, a similar relationship between entanglement density and strain hardening is suggested for semicrystalline polymers as found for amorphous polymers. The crystalline domains have a viscous contribution but no entropic network contribution at large strains.

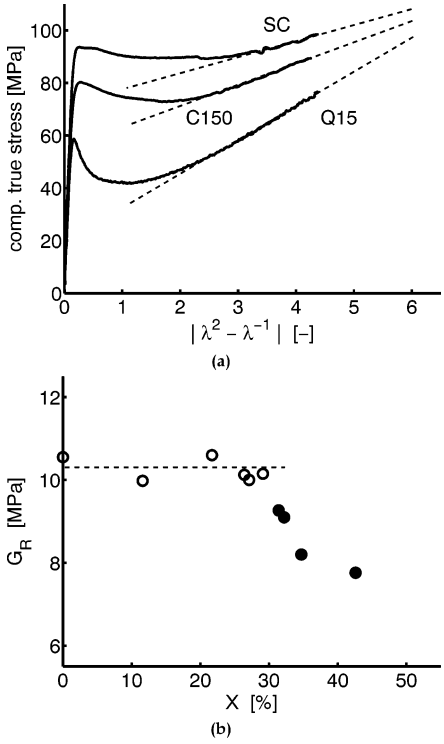

Figure 3. Compressive behavior of PET samples crystallized with different nonisothermal procedures as given in Table 2 (a) and strain hardening modulus G_R of all PET samples vs degree of crystallinity χ (b). Filled symbol represents C and SC samples and open symbols Q15 and IC samples.

The maximum degree of crystallinity obtained by isothermal crystallization was approximately 30%, but higher levels were measured for the slowly cooled samples given in Table 2. In Figure 3a the compression curves with its strain hardening (dashed line) are given for several of these nonisothermal crystallization procedures: cooled in the press at 15 °C (Q15) and 150 °C (C150) and switching of the heating of the press (SC). In Figure 3b the strain hardening moduli are plotted against the degree of crystallinity for all PET samples tested. The postulated hypothesis, that crystallinity has no contribution to the strain hardening modulus, seems to be invalid at first sight from Figure 3b since the strain hardening modulus decreases above a certain degree of crystallinity. However, it should be considered that the samples with the higher crystallinity were obtained from the nonisothermal crystallization procedures (C and SC), indicated in Figure 3b with the filled symbols. The strain hardening modulus is found to decrease with decreasing cooling rate (Figure 3a). An explanation originates from the fact that crystallization from the melt allows for rearrangement of the chains during chain folding. This "reeling in" of chains during crystallization leads to disentanglement of the chains from the melt,[36−38] more pronounced for lower cooling rates, resulting in a lower entanglement density and consequently a lower strain hardening modulus. On the other hand, when isothermal annealing temperatures are applied, the chain mobility is sufficient for the crystallites to grow but not sufficient to disentangle amorphous polymer coils, and hence strain hardening is preserved. Similar trends in the effect of entanglement density, caused by different crystallization processes, on the strain hardening behavior were already

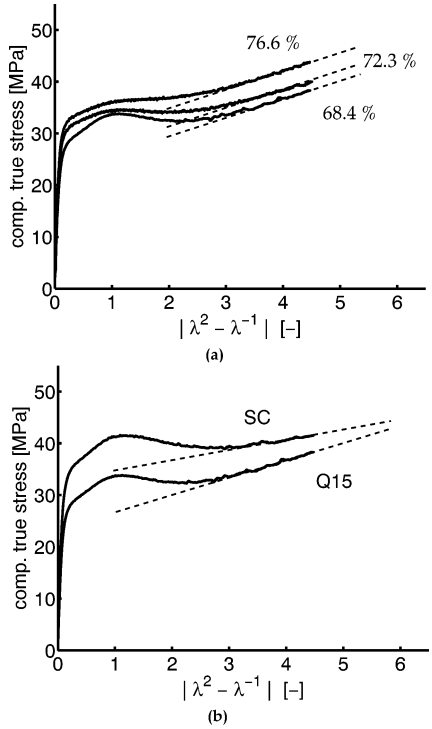

Figure 4. Compressive behavior of (a) isothermally crystallized PE-1 samples, having different degree of crystallinity (χ), and (b) PE-1 samples crystallized with different nonisothermal procedures.

mentioned in the Introduction, regarding the observations in the study on polyethylene films of UHMW-PE.[16,17] Here a more pronounced effect of entanglement density on strain hardening can be found in comparing melt crystallized and solution crystallized UHMW-PE samples, where the first exhibits a large strain hardening, due to the large entanglement density, and the latter shows almost no strain hardening, since entanglement density is extremely low. Partial recrystallization of the solution crystallized samples results in intermediate level of strain hardening,[17] and complete remelting shows the reversibility of the mechanism, indicating the relation with number of entanglements rather than molecular constitution.[39] Similar trends in drawability, dependent on entanglement density, were also found in the comparison of slow cooled samples with quenched samples of melt crystallized polyethylene.[14]

HDPE. The intrinsic compression behavior of several PE-1 samples is shown in Figure 4. In Figure 4a the compressive stress−strain relation is plotted for three samples with different crystallinity, obtained from isothermal (annealing) procedures, and in Figure 4b the behavior is plotted for different nonisothermal crystallization procedures. Figure 5 shows the resulting strain hardening modulus of all PE-1 samples tested. Similar trends as for the PET samples are found since the strain hardening modulus does not depend on crystallinity when isothermal annealing is applied and only seems to drop when a sample is slowly cooled (crystallized) from the melt. It is interesting to note that the highest degree of crystallinity of the annealed PE-1 sample (IC125h48) is of the same level as the slowly crystallized (IC) PE-1 sample, which proves that the drastic decrease in strain hardening modulus of the latter can only be explained by the type of crystallization procedure and not by crystallinity itself.

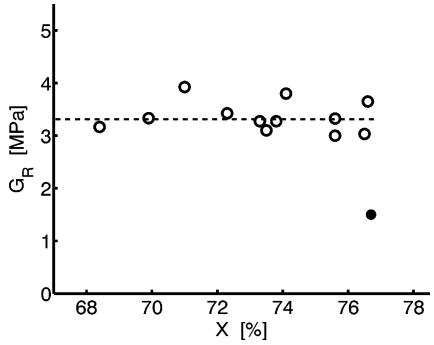

Figure 5. Strain hardening modulus, G_R, of PE-1 samples vs degree of crystallinity (χ). Filled symbol represents SC samples and open symbols Q15 and IC samples.

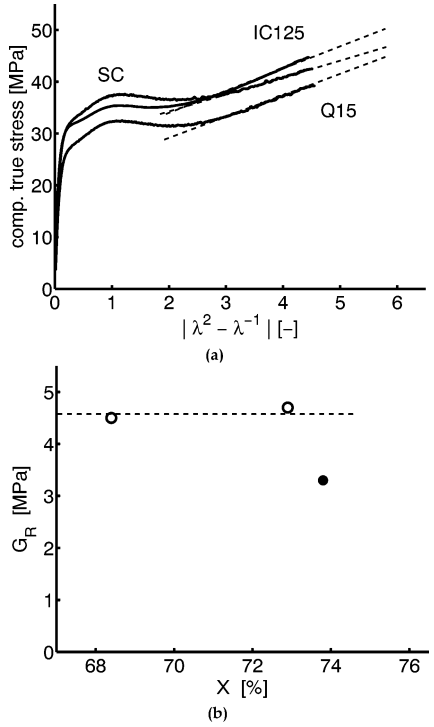

Figure 6. Compressive behavior of PE-2 samples crystallized with different procedures as given in Table 2 (a) and strain hardening modulus G_R of these PE-2 samples vs degree of crystallinity χ (b). Filled symbol represents SC samples and open symbols Q15 and IC samples.

For the different samples of the higher molecular weight grade (PE-2), again the strain hardening modulus only drops when the sample is cooled slowly from the melt and not upon annealing of the sample, as can be seen in Figure 6. Another observation favorable for the relation between entanglement density and strain hardening arises by comparing Figures 5 and 6b. It is found that the strain hardening modulus of the higher molecular weight PE-2 samples are larger and that the drop in strain hardening by slowly cooling from the melt is lower than for the lower molecular weight sample PE-1.

A high molecular weight polymer is likely to have a higher chain entanglement density for both crystallization procedures, since "reeling in" of the long chains is more difficult, because of a relatively higher viscosity related to molecular weight.

The increase in entanglement density and the decreasing difference effected by cooling rate for increasing molecular weight was also observed in the investigation

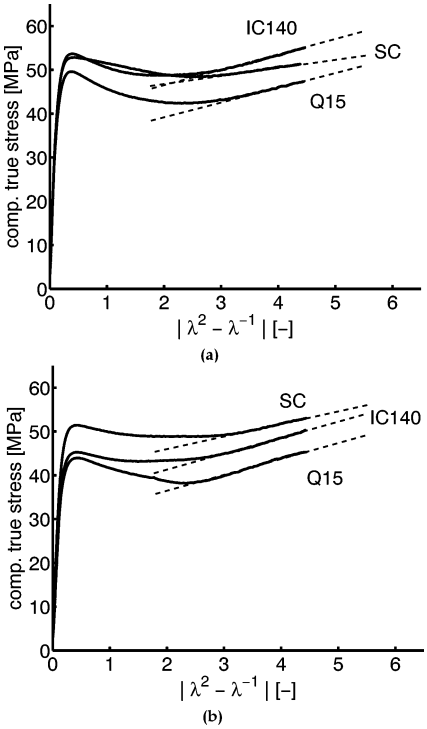

Figure 7. Compressive behavior of PP-1 (a) and PP-2 (b) samples crystallized with different procedures as given in Table 2.

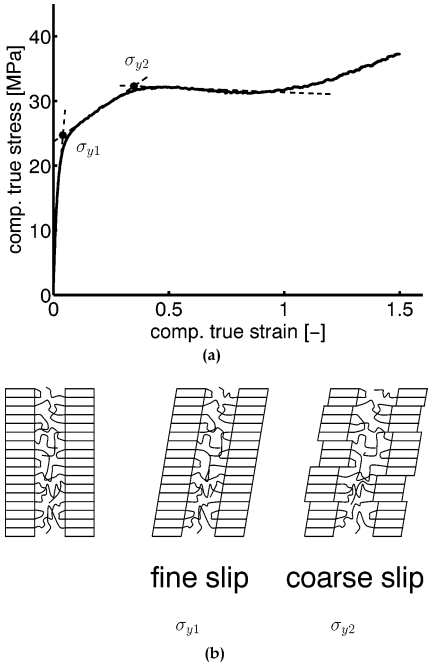

Figure 8. Observation of first (σ_{y1}) and second (σ_{y2}) yield stress in HDPE (a) and schematic representation of fine chain slip at the first yield stress followed by coarse chain slip at the second yield point.

of natural draw ratio.[14] Similar trends in the effect of molecular weight and cooling rate on the strain hardening behavior were also found in the literature.[18−20] In these studies no influence of supermolecular structure was observed, e.g., spherulitic size and structure. The observed differences were attributed to level of crystallinity.[20] The effect of cooling rate was only observed indirectly in ref 19 since they used tensile experiments, where brittle failure was observed for the lower molecular weight, slowly cooled samples. In macroscopic tensile behavior localization and failure phenomena cannot be overcome as in the compressive measurements of this study. The relation between intrinsic strain hardening and macroscopic tensile behavior will be discussed in the following section.

PP. Figure 7 shows the results of compression tests on the PP samples. Similar to the PET and PE samples, the strain hardening decreases whenever the samples are slowly crystallized from the melt (SC) compared to quenching from the melt (Q15) and stays at the same level when the samples are annealed. Also similar to the observation in the two molecular weight grades of PE is that the decrease upon slow crystallization is more pronounced for the lower molecular weight polymer grade and that the difference in yield stress between the quenched and annealed low molecular weight PP sample (PP-1) is less than for the higher molecular weight PP samples (PP-2) due to the higher mobility of the lower molecular weight polymer.

The measured strain hardening Moduli for the PE ($G_R \approx 1.6-4.6$ MPa) and PP ($G_R \approx 2.2-3.9$ MPa) samples correspond with those found by Haward (PE: $G_R \approx 1.7-4.4$ MPa; PP: $G_R \approx 4.1$ MPa).[11] A conclusion that can be drawn from the results in this study, obtained from three different semicrystalline polymers, is that strain hardening of semicrystalline polymers can be described with a neo-Hookean relation originating from the rubber-elasticity theory, which is also valid for amorphous polymers. There is no observation of any contribution of the crystalline domains to the strain hardening, and an indication toward a relationship with entanglement density exists. For this reason, it can be assumed that studies relating crystallinity to strain hardening are ambiguous when investigation of this relationship is based on different polymer grades, e.g., ref 13. Also, experimental work, using different crystallization techniques, should be discussed carefully, taking in mind the effect of crystallization rate on overall entanglement density.

3.4. Yield Stress. The observations of the compressive behavior of all tested samples already showed an increase in yield stress with an increasing degree of crystallinity. Since the experiments were performed at room temperature, and PET is situated in the glassy state, the changes in the yield stress of PET have to be contributed to both a change of the crystalline yield stress and the amorphous yield stress. In PP softening was observed, so here an amorphous contribution is also present at the applied deformation rate and temperature. This coupling between amorphous and crystalline yield stress brings an extra parameter in investigating the relation between yield stress and crystallinity.

Therefore, a further investigation of this relation is only performed for HDPE, with its glass transition temperature far below room temperature, resulting in a rubberlike behavior (no yielding) of the amorphous phase. Regarding yielding, two characteristics can be distinguished: the existence of two yield points (double yield) and the relation between crystallinity and yield stress. In this study, all PE samples tested showed the existence of double yield (see Figure 8a). Time-resolved small- and wide-angle X-ray experiments were performed by Butler et al.[40−43] during deformation of PE in both tensile[40,41,43] and compression tests,[42] and they concluded that double yield exists in both deformation modes. Further occurrence of double yield has been reported mainly in engineering stress−strain curves.[44−46]

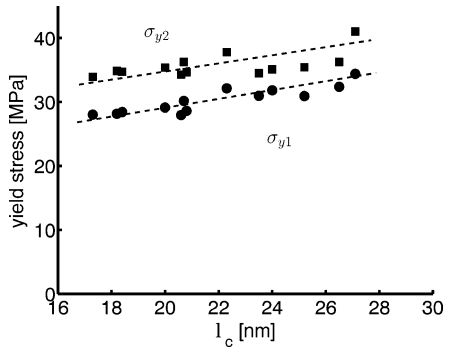

Figure 9. Relationship between lamellar thickness (l_c) and the two yield stresses of the tested HDPE samples.

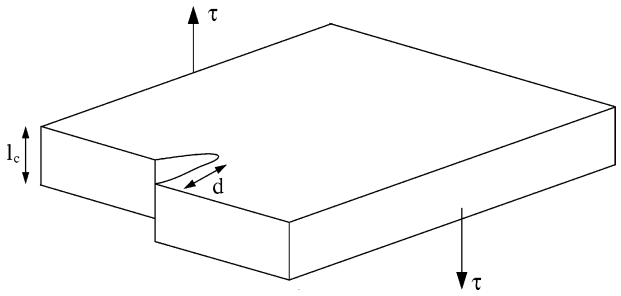

Figure 10. Schematic representation of a screw dislocation in a lamella.

The deformation mechanisms of both yield points are generally associated as fine chain slip combined with a martensitic type of transformation within the lamellae at the first yield point and a process of coarse chain slip resulting in lamellar fragmentation at the second yield point,[41−43,47] as schematically presented in Figure 8b.

A proper model for the relation between crystallinity and level of yield stress does not yet exist. Most of the previous studies find the crystal lamellae thickness to be the controlling parameter in the activation of yield in polyethylene[18−20,23−27] and polypropylene.[28,29] Figure 9 gives both yield stresses, determined as shown in Figure 8a, as a function of lamellar thickness. Independent of the type of crystallization procedure applied, a proportionality is found between lamellar thickness and yield stress, indicating that both yield stresses are activated by similar mechanisms. The most commonly used model that describes the yield stress dependence of lamellar thickness is the one first proposed by Young,[22] later refined by Shadrake and Guiu.[48] This model assumes that yield involves the thermal activation of screw dislocation with the burgers vector parallel to the chain axis.

A schematic representation of a screw dislocation with a Burgers vector b and growth over a distance d from the edge is given in Figure 10, where l_c is the crystal thickness and τ is the applied shear stress. According to the theory developed, the change in Gibbs free energy, ΔG, associated with the formation of such a dislocation is given by

$$\Delta G = E - W = \frac{l_c K b^2}{2\pi} \ln \frac{d}{r_0} - l_c d\tau b \qquad (6)$$

Here the first term (E) relates to the elastic strain energy, with r_0 being the core radius of the dislocation, b the Burgers vector at distance d from the edge of the crystal, l_c the crystal thickness, and K a function of the crystalline shear modulus. The second term (W) relates to the work performed by external shear forces, expressed in the shear stress τ applied. A dislocation will be activated for a critical value d_c obtained from the maximum in ΔG, resulting in

$$d_c = \frac{Kb}{2\tau\pi} \qquad (7)$$

In this approach a core energy contribution is neglected. Recently Brooks and Mukhtar[27] modified the model, including an extra term representing the core energy (E_0) in eq 6. Another adjustment, when applying the model to polyethylene, is that the chain axis, and therefore the Burgers vector, lies at a tilted angle of approximately 34.5° to the fold surface normal.[49] The lamellar thickness l_c in eq 6 is better replaced by the stem length, l. From these adjustments the following equation results:

$$\Delta G = E + E_0 - W = \frac{lKb^2}{2\pi} \ln \frac{d}{r_0} + E_0 - ld\tau b \qquad (8)$$

All authors[22−24,27,48] assumed that a Tresca yield criteria is valid, i.e., $\sigma_y = 2\tau$, and combining eq 7 with eq 8 resulted in the following expression for the yield stress:

$$\sigma_y = \frac{K}{\pi}\alpha(T) \exp\left[-\frac{2\pi\Delta G_c}{lKb^2} + 1\right] \qquad (9)$$

where

$$\alpha(T) = \frac{b}{r_0} \exp\left[\frac{2\pi E_0}{Klb^2}\right] \qquad (10)$$

The Gibbs free energy, ΔG_c, is assumed to be in the range $40kT-60kT$,[48] with k the Boltzmann constant and T the absolute temperature. Taking a value for G_c of $60kT$, Brooks and Mukhtar[27] used this approach to fit an optimal value for the temperature-dependent parameter, $\alpha(T)$, for a range of polyethylene grades and found a linear relation for $\alpha(T)$ for a strain rate of 10^{-2} s^{-1}. The value of K, taken as a geometric mean of the shear modulus, $(C_{44}C_{55})^{0.5}$, is also dependent on temperature and was taken from theoretical work by Karasawa et al.[50] Further, the value for the Burgers vector, b, is generally suggested to be the value of the c-axis of the polyethylene unit cell, being 2.54 Å, and r_0 is thought to be on the order of $2b$. Applying the theory to the results of this study, taking $\alpha(T) = 0.1481$ obtained from ref 27 and $K = 2.359$ GPa taken from ref 50 for the involved temperature of 22 °C (=295 K), shows a relation between stem length within the lamellae and yield stress as indicated in Figure 11 by the dashed lines, using a value of ΔG_c of respectively $40kT$ and $60\ kT$.

The calculated values of the yield stress as a function of lamellar thickness are in fair agreement with the experimental results of the first yield stress. The second yield stress can only be fitted by using a value of ΔG_c lower than $40\ kT$, which is, however, incorrect since a lower value than $40kT$ is not realistic,[48] especially considering the fact that the strain rate is constant and low (3×10^{-3} s^{-1}) in the applied compression test. This observation doubts the validation of Young's slip model for the second yield point. Moreover, the second yield

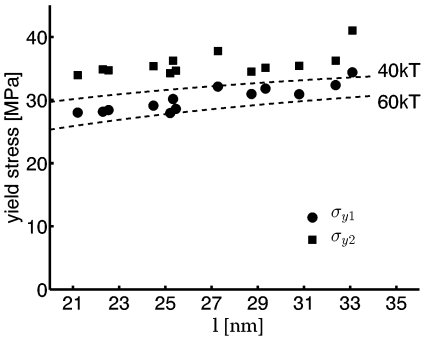

Figure 11. Relationship between first (circles) and second (squares) yield stress and stem length (l) of tested HDPE samples. The dashed lines represent the theoretical calculated values, taking for ΔG_c $40kT$ and $60kT$.

point is considered to be associated with lamellar fragmentation, which is a heterogeneous and irreversible deformation mode.[40−45] Furthermore, it should be emphasized that the current selections of b, K, and α-(T) (r_0 and E_0) are taken from literature, where also some inconsistency in these values was found; no further attempts were made to fit these parameters to match the experimental results. The reason is that, apart from our own criticism of the model, other indications for the notion that the above-described model is not perfectly reliable result from the observation that, for example, fold surface morphology also seems to effect the yield behavior.[51] In the investigation of double yield in polyethylene, some authors[46,52] discussed the observed temperature or strain rate dependence of double yield in terms of viscoelastic (α) relaxation in the crystals. A combination of the kinetic aspects of α-relaxation and the dislocation model presented above looks a promising route.[30] Another indication for the suggestion that α-relaxation should be considered in the explanation for plastic flow results from the deformation behavior of oriented UHMW-PE fibers.[53] The irreversible, plastic flow contribution in the deformation was here related to translational motion of chains within the crystal, which is governed by a fast exchange in gauche defects and is accepted to be the origin of the α-transition in polyethylene.[53−55] A detailed investigation in the effect of temperature and strain rate is necessary to draw further conclusions and is beyond the scope of this work.

4. Conclusions

Uniaxial compression tests proved to be a successful method for characterization of large strain deformation at room temperature of semicrystalline polymers, regardless of their glass transition temperature. Annealing of quenched samples was shown to have a significant effect on the degree of crystallinity and lamellar thickness. For poly(ethylene terephthalate) the degree of crystallinity was in the range between 0% and 30% and for polyethylene in the range of 68−76% upon applying isothermal crystallization procedures, but for both polymers no effect of annealing on the strain hardening modulus at large strains ($\lambda \sim 2$) was observed. Long time annealing at high temperature, but still below the melting temperature, of polyethylene resulted in a crystallinity equal to the crystallinity obtained when a slow crystallization process from the melt was applied. The slow crystallization (slow cooling) procedures from the melt resulted in a lower strain hardening modulus for all polymers tested. However, the decrease in strain hardening, if present, is dependent on the molecular weight and is less for the higher molecular weight polymers. Considering the effect of cooling rate in the crystallization process of a high or low viscous melt, on the number of trapped entanglements in the solidified polymer, strain hardening is expected to be proportional to entanglement density, irrespective of the degree of crystallinity. This relationship between strain hardening and entanglement density is in analogy with a rubber-elastic response. From the fact that a neo-Hookean description indeed holds for all results in this study, it can be concluded that strain hardening primarily depends, at least at large strains, on entanglement density. The absence of crystallites acting as physical cross-links leads to the suggestion that, after yielding, crystallites have a high mobility. The yield stress at which slip of crystalline lamellae is reached was shown to be dependent on crystallinity or better lamellar thickness. A fair correlation was obtained between the measured yield stress in polyethylene and that predicted by a mechanism involving the nucleation and propagation of screw dislocations, as found in the literature. Still, we think an investigation of the activation of yielding with a kinetic approach, considering the role of stress on the α-relaxation chain mobility, is justified.

Acknowledgment. The authors acknowledge Ronald Schellekens of DSM Research for his support and supply of materials, Wim Bras for the availability of the X-ray facilities at the Dubble beamline at the European Synchrotron Radiation Facility (ESRF, Grenoble, France), and the financial support provided by the Dutch Polymer Institute (DPI) (project 164).

References and Notes

(1) Takayanagi, M.; Imada, K.; Kajiyama, T. *J. Polym. Sci., Part C* **1966**, *15*, 263−80.
(2) Halpin, J. C.; Kardos, J. L. *J. Appl. Phys.* **1972**, *43*, 2235−41.
(3) G'Sell, C.; Jonas, J. J. *J. Mater. Sci.* **1981**, *16*, 1956−74.
(4) G'Sell, C.; Hiver, J. M.; Dahoun, A.; Souahi, A. *J. Mater. Sci.* **1992**, *27*, 5031−9.
(5) Haward, R. N.; Thackray, G. *Proc. R. Soc. London A* **1967**, *302*, 453−72.
(6) Haward, R. N. *Polymer* **1994**, *35*, 3858−62.
(7) Tervoort, T. A.; Govaert, L. E. *J. Rheol.* **2000**, *44*, 1263−77.
(8) van Melick, H. G. H.; Govaert, L. E.; Meijer, H. E. H. *Polymer* **2003**, *44*, 2493−502.
(9) Haward, R. N. *Trans. Faraday Soc.* **1942**, *38*, 394−403.
(10) Govaert, L. E.; Tervoort, T. A. *J. Polym. Sci., Part B: Polym. Phys.* **2004**, *42*, 2041−9.
(11) Haward, R. N. *Macromolecules* **1993**, *26*, 5860−9.
(12) Takayanagi, M.; Nitta, K. *Macromol. Theory Simul.* **1997**, *6*, 181−95.
(13) Hiss, R.; Hobeika, C. L.; Strobl, G. *Macromolecules* **1999**, *32*, 4390−403.
(14) Capaccio, G.; Gibson, A. G.; Ward, I. M. In *Ultra-High Modulus Polymers*; Ciferri, A., Ward, I. M., Eds.; Applied Science Publ.: London, 1979; p 1.
(15) Smith, P.; Lemstra, P. J. *Br. Polym. J.* **1980**, *12*, 212−4.
(16) Smith, P.; Lemstra, P. J.; Booij, H. C. *J. Polym. Sci., Part B: Polym. Phys.* **1981**, *19*, 877−888.
(17) Smith, P.; Lemstra, P. J. *Colloid Polym. Sci.* **1980**, *258*, 891−4.
(18) Kennedy, M. A.; Peacock, A. J.; Failla, M. D.; Lucas, J. C.; Mandelkern, L. *Macromolecules* **1995**, *28*, 1407−21.
(19) Kennedy, M. A.; Peacock, A. J.; Mandelkern, L. *Macromolecules* **1994**, *27*, 5297−5310.
(20) Popli, R.; Mandelkern, L. *J. Polym. Sci., Part B: Polym. Phys.* **1987**, *25*, 441−83.
(21) Flory, P. J.; Yoon, D. Y. *Nature (London)* **1978**, *272*, 226−9.
(22) Young, R. J. *Philos. Mag.* **1974**, *30*, 85−94.
(23) Young, R. J. *Mater. Forum* **1988**, *11*, 210−16.

(24) Crist, B.; Fisher, C. J.; Howard, P. R. *Macromolecules* **1989**, *22*, 1709−18.
(25) Darras, O.; Séguéla, R. *J. Polym. Sci., Part B: Polym. Phys.* **1993**, *31*, 759−66.
(26) Brooks, N. W.; Ghazali, M.; Duckett, R. A.; Unwin, A. P.; Ward, I. M. *Polymer* **1998**, *40*, 821−5.
(27) Brooks, N. W. J.; Mukhtar, M. *Polymer* **2000**, *41*, 1475−80.
(28) O'Kane, W. J.; Young, R. J. *J. Mater. Sci., Lett.* **1995**, *14*, 433−5.
(29) O'Kane, W. J.; Young, R. J.; Ryan, A. J. *J. Macromol. Sci., Phys.* **1995**, *B34*, 427−58.
(30) Séguéla, R. *J. Polym. Sci., Part B: Polym. Phys.* **2002**, *40*, 593−601.
(31) Fischer, E. W.; Schmidt, G. F. *Angew. Chem.* **1962**, *74*, 551−62.
(32) van der Burgt, F. P. T. J.; Rastogi, S.; Chadwick, J. C.; Rieger, B. *J. Macromol. Sci., Phys.* **2002**, *B41*, 1091−1104.
(33) Young, R. J.; Lovell, P. A. *Introduction to Polymers*; Stanley Thornes (Publishers) Ltd.: London, 1991.
(34) Van Krevelen, D. W. *Properties of Polymers*, 3rd ed.; Elsevier: Amsterdam, 1994.
(35) Boyce M. C.; Haward R. N. In *The Physics of Glassy Polymers*, 2nd ed.; Haward, R. N., Young, R. J., Eds.; Chapman & Hall: London, 1997; Chapter 5.
(36) DiMarzio, E. A.; Guttman, C. M.; Hoffman, J. D. *Faraday Discuss.* **1979**, *68*, 210−17.
(37) Hoffman, J. D. *Polymer* **1982**, *23*, 656−70.
(38) Peterlin, A. *Macromolecules* **1980**, *13*, 777−82.
(39) Bastiaansen, C. W. M.; Meijer, H. E. H.; Lemstra, P. J. *Polymer* **1990**, *31*, 1435−40.
(40) Butler, M. F.; Donald, A. M.; Ryan, A. J. *Polymer* **1997**, *38*, 5521−38.
(41) Butler, M. F.; Donald, A. M.; Ryan, A. J. *Polymer* **1998**, *39*, 39−52.
(42) Butler, M. F.; Donald, A. M.; Ryan, A. J. *Polymer* **1998**, *39*, 781−92.
(43) Butler, M. F.; Donald, A. M.; Bras, W.; Mant, G. R.; Derbyshire, G. E.; Ryan, A. J. *Macromolecules* **1995**, *28*, 6383−93.
(44) Brooks, N. W.; Duckett, R. A.; Ward, I. M. *Polymer* **1992**, *33*, 1872−80.
(45) Brooks, N. W.; Unwin, A. P.; Duckett, R. A.; Ward, I. M. *J. Macromol. Sci., Phys.* **1995**, *B34*, 29−54.
(46) Séguéla, R.; Darras, O. *J. Mater. Sci.* **1994**, *29*, 5342−52.
(47) Bowden, P. B.; Young, R. J. *J. Mater. Sci.* **1974**, *9*, 2034−51.
(48) Shadrake, L. G.; Guiu, F. *Philos. Mag.* **1976**, *34*, 565−81.
(49) Bassett, D. C.; Hodge, A. M. *Proc. R. Soc. London A* **1978**, *359*, 121−32.
(50) Karasawa, N.; Dasgupta, S.; Goddard, W. A. *J. Phys. Chem.* **1991**, *95*, 2260−72.
(51) Sirotkin, R. O.; Brooks, N. W. *Polymer* **2001**, *42*, 3791−97.
(52) Gaucher-Miri, V.; Séguéla, R. *Macromolecules* **1997**, *30*, 1158−67.
(53) Govaert, L. E.; Lemstra, P. J. *Colloid Polym. Sci.* **1992**, *270*, 455−64.
(54) Boyd, R. H. *Polymer* **1985**, *26*, 323−47.
(55) Boyd, R. H. *Polymer* **1985**, *26*, 1123−33.

MA035279T